

Sensor and Simulation Notes

Note 565

June 2013

Improved Feed Design for Enhance Performance of Reflector Based Impulse Radiating Antennas

Dhiraj K. Singh¹, D. C. Pande¹, and A. Bhattacharya², Member, *IEEE*

¹Electronics & Radar Development Establishment, Bangalore, India

²Indian Institute of Technology, Kharagpur, India

Abstract—Conventional reflector based Impulse Radiating Antennas (IRA's) are designed with conical taper transmission line feed. A novel feed design approach is used to enhance gain of the IRA without increasing diameter of the reflector. This paper discuss conventional and new IRA designs of different input impedances. IRA with conventional feed and with new dipole feed is designed for both 200 Ω and 100 Ω input impedance category. The IRA with new feed design offers better gain compared to conventional IRA for both 200 Ω and 100 Ω input impedance category. These antenna designs are analyzed using the Finite Difference Time Domain (FDTD) method and the result obtained shows that IRAs with new dipole feed offers better gain than IRAs with conventional feed for respective input impedance category without any compromise in time domain characteristics. A half IRA with new feed with input impedance of nearly 50 Ω was realized and measured to establish the advantage of new dipole feed IRA.

Index Terms— ACD, BALUN, FDTD, IRA, UWB

1. INTRODUCTION

Impulse Radiating antennas are gaining lots of attention for ultra-wideband (UWB) Radar Applications due to their large instantaneous bandwidth and pulse fidelity. The spherical wave that propagates through the transmission line feed is converted to the plane wave by the parabolic reflector. One of the commonly used IRA consists of a parabolic reflector fed by a conical transverse electromagnetic (TEM) transmission line. The conventional Impulse Radiating Antennas [1]-[6] had been designed for 200 Ω input impedance wherein the conical plate transmission line feed used is of 400 Ω as shown in Fig. 1. An alternate feed design and optimum arm separation for improved antenna efficiency was suggested in the past [7,8].

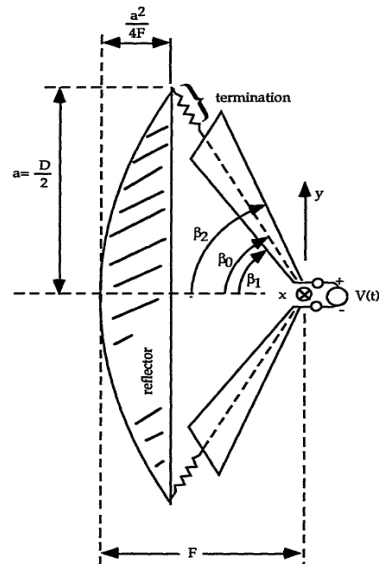


Fig. 1 Schematic of Conventional IRA

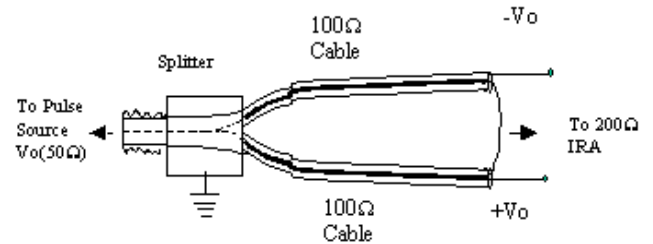


Fig. 2 Balun Configuration

The commonly used sources and measuring instrumentations have an unbalanced coaxial output with a 50Ω source resistance, a 50Ω to 200Ω balun is used to connect standard sources and instrumentations to the 200Ω input of IRA. The commonly used balun [9] for IRA consists of two 100Ω coaxial cable connected in parallel at source end and in series at IRA feed end as shown in Fig. 2. The 100Ω cables like RG-213 and its equivalents are not commonly available, hence it limits the wide use of the IRA for different applications. A similar situation existed in the TV reception in earlier days, where due to non-availability of 73Ω twin lead feeder line, the dipole was folded to match with 400Ω lines. The idea of using asymptotic conical dipole (ACD) as feed for reflector IRA was introduced in [15] and ideal ACD profile suitable as feed for IRA was suggested. Here, attempt is made to compare time domain and frequency domain performance of ACD feed IRA with conventional IRA for different input impedance category. This paper describes application of full and half section of asymptotic conical dipole as feed for reflector IRA for 100Ω and 200Ω input impedance respectively. It compares the analysis results of conventional and new IRA and shows that new feed is slimmer than the conventional feed for respective input impedance category and the new IRAs offers higher gain than corresponding conventional IRAs. In Section 2 of this paper, the design of conventional IRA of 200Ω and 100Ω input impedance is presented. The design of new feed IRA for 200Ω and 100Ω input impedance category is discussed in Section 3. Finite Difference Time Domain (FDTD) analysis of New and Conventional IRAs are compared and measured results are elaborated in Section 4. Discussion and conclusion are presented in Section 5 & 6 respectively.

2. CONVENTIONAL IRA DESIGN

The Schematic of conventional IRA is shown in Fig. 1. It consists of a conical transmission line structure feeding into and attaching to a parabolic reflector. Suitable loads are placed between the transmission line feed and the dish in order to reduce reflections and provide the matched load required of the BTW (balanced transmission line wave). Typically, in an IRA, two 400 Ω conical plate lines are connected in parallel at the feed point to get 200 Ω input impedance. The reason for choosing a 400 Ω line is to get a smaller cone angle for the transmission line thereby reducing the aperture blockage and, in turn, achieving a better antenna gain and reduced weight of the antenna. A 100 Ω input impedance IRA is designed using conventional two 200 Ω conical taper line connected in parallel at the feed point. The design parameters of the 200 Ω conical lines is calculated as per [6] and design values are tabulated in Table.1. The 100 Ω conical line fed IRA design is not commonly used because of wider profile of the conical feed arm. Here 100 Ω IRA is designed and analyzed to compare the results with corresponding new IRA in subsequent section. The design parameters of the conventional IRA for 200 Ω and 100 Ω input impedance are given below in Table 1. The feeding line is aligned 45⁰ from the vertical axis and terminating resistors each of 200 Ω for design of Fig. 3 and 100 Ω for design of Fig. 4 is placed between end of the dipole and reflector. The dimension of the feeding dipole and the design of both 200 Ω and 100 Ω conventional IRA is depicted in Fig. 3 and Fig. 4 respectively.

Table 1: Antenna parameters for Conventional IRAs

Sl.No.	Antenna parameters	Relation	Design values for 200 Ω IRA	Design values for 100 Ω IRA
1.	Reflector diameter	D	0.46 m	0.46 m
2.	Focal length	F	0.18 m	0.18 m
3.	$F_d = F/D$	F_d	0.3913	0.3913
4.	Number of arms		4	4
5.	Arm configuration		90 ⁰	90 ⁰
6.	Impedance, Z_c	Z_c	200 Ω	100 Ω
7.	Geometrical factor, F_g	$F_g = Z_c/Z_o$, $k=0.7513$	1.061	0.5305
8.	β_o (Fig.1)	$\beta_o = \arctan(1/(2 * F_d - (1/8 F_d)))$	65.14 ^o	65.14 ^o
9.	β_1 (Fig.1)	$\beta_1 = 2 \arctan(\sqrt{k} * \tan(\beta_o/2))$	57.94 ^o	32.36 ^o
10.	β_2 (Fig.1)	$\beta_2 = 2 \arctan(\tan(\beta_1/2)/k)$	72.77 ^o	109.17 ^o
11.	$\beta_2 - \beta_1$ (Fig.1)	2α	14.83 ^o	76.814 ^o

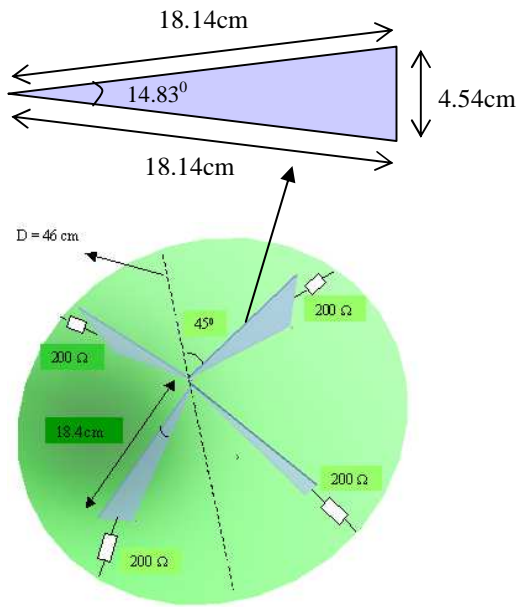


Fig. 3 Conventional IRA design ($Z_{in} = 200 \Omega$)

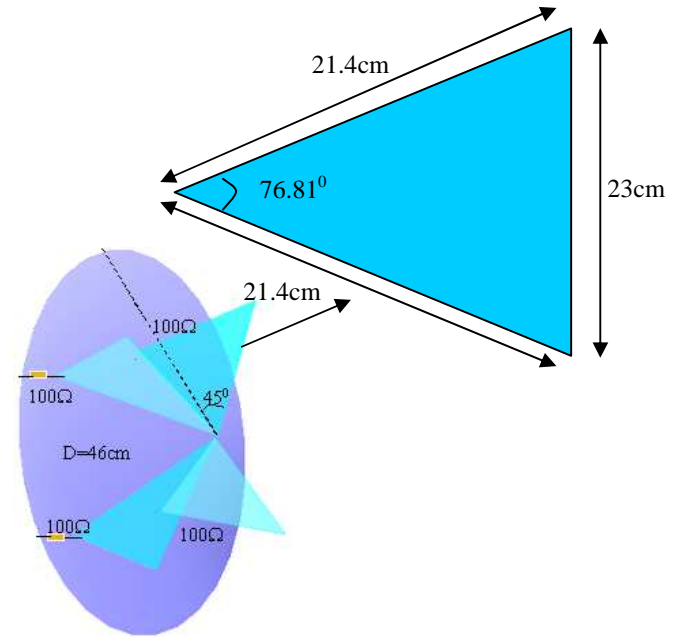


Fig. 4 Conventional IRA design ($Z_{in} = 100 \Omega$)

3. NEW FEED IRA DESIGN

New IRA is designed using asymptotic conical dipole (ACD) as feeding TEM line and 46 cm paraboloidal reflector. The ACD feed profile is derived using equivalent charge method with only equivalent line charge $\lambda(z)$ as suggested in [15]. The charge distribution is defined to be rotationally symmetric about z -axis with opposite charge reflected about the symmetry plane (x - y plane) as shown in Fig. 5. The equivalent line charge $\lambda(z)$ on the z -axis be given by [12]:

$$\lambda(z) = \begin{cases} \lambda_0, & 0 < z < z_0 \\ -\lambda_0, & 0 > z > -z_0 \\ 0, & z = 0, z > z_0 \end{cases} \quad (1)$$

where mean charge separation $z_0 > 0$, charge density $\lambda_0 > 0$

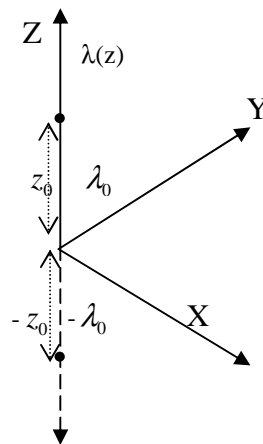


Fig. 5 Charge distribution

In order to generate the ACD profile, potential distribution due to $\lambda(z)$, at any point $P(r, \varphi, z)$ is equated to surface potential function of infinite biconical structure. The (z, r) coordinates for the asymptotic conical profiles are given in terms of Θ_0 as

$$\Theta_0^{-2} = \frac{\left[z + \sqrt{z^2 + r^2} \right]^2}{\left[z + z_0 + \sqrt{(z + z_0)^2 + r^2} \right] \left[z - z_0 + \sqrt{(z - z_0)^2 + r^2} \right]} \quad (2)$$

where, $\Theta_0 = \tan\left(\frac{\theta_0}{2}\right)$

where, Θ_0 is a constant determined by the desired asymptotic impedance from the infinite biconical surface. For each value of z between zero and the antenna height h , there exists a unique element radius r . Eq. (2) was solved numerically using Newton-raphson method to get the contour of asymptotic element as shown in Fig. 6. The flat surface obtained by the ACD contour and vertical axis of Fig. 6 is one pole of the dipole. Two of these surfaces forms a dipole known as half section of ACD and the mirror image of half section of ACD along the vertical axis gives full section ACD as shown in Fig. 7.

The characteristic impedance of loss-less transmission line is proportional to square root of the ratio of inductance and capacitance, following this premise the input impedance of ACD full section should be half of the ACD half section because capacitance increased twice and inductance reduced to half compared to ACD half section.

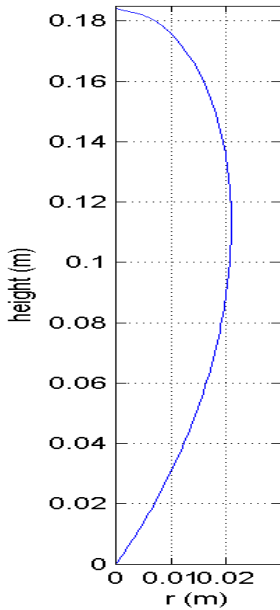


Fig. 6 ACD Contour

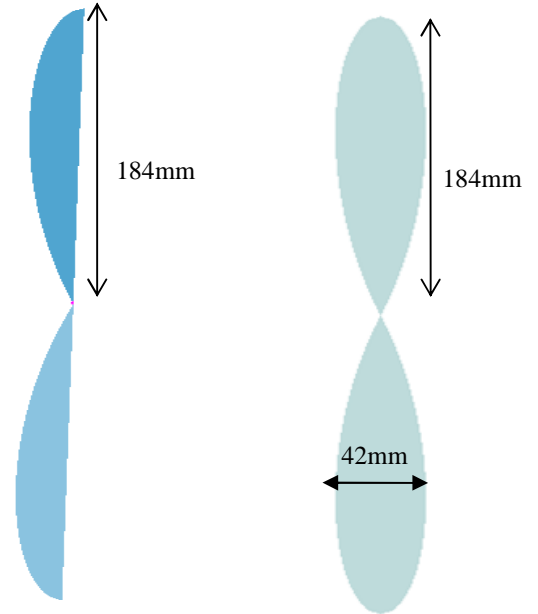


Fig. 7 ACD half & full section

3. FDTD ANALYSIS AND MEASUREMENT

Half section of ACD, full section of ACD is analyzed in time domain using the finite difference time domain solver XFDTD (v7.1). The excitation waveform used for the simulation is a gaussian pulse of amplitude ~ 0.56 volts, FWHM ~ 50 ps and rise time ~ 50 ps as shown in Fig. 8. The absorbing boundary condition with seven perfectly matched layers (PML) is used for this simulation. The input impedance obtained from analysis shown in Fig. 9 shows that input impedance of ACD full section reduces to nearly half across the frequency range.

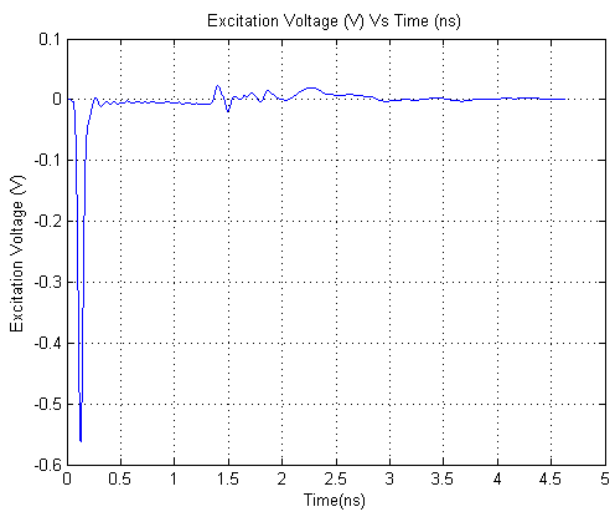


Fig. 8 Excitation waveform used for FDTD simulation

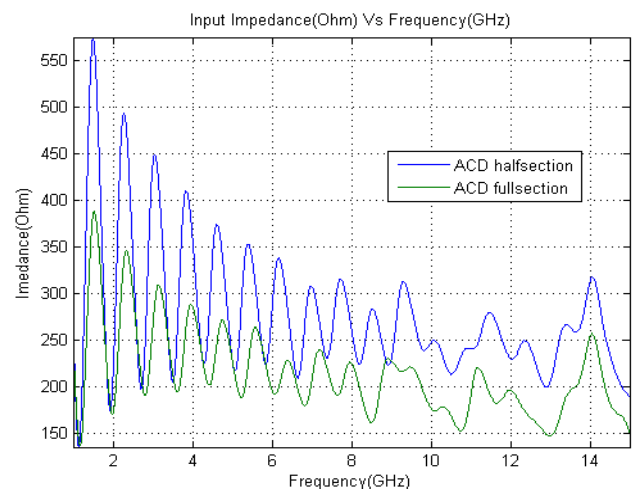


Fig. 9 Input impedance of ACD half & full section

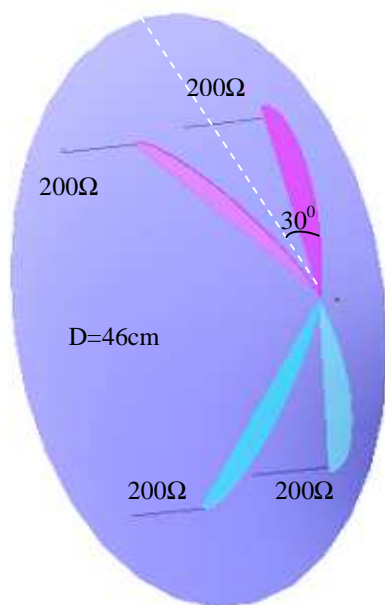


Fig. 10 New IRA (Input Impedance 200 Ω)

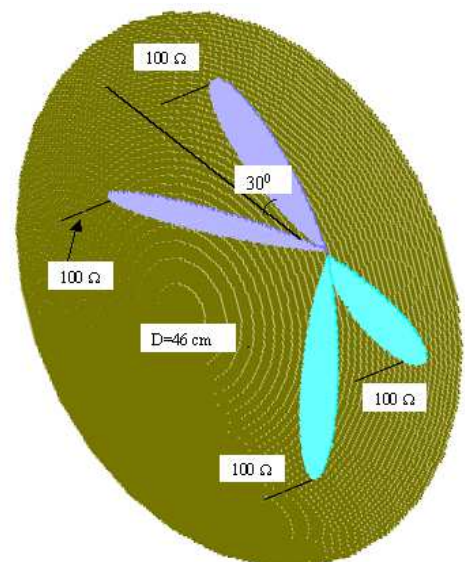


Fig. 11 New IRA (Input Impedance 100 Ω)

The analysis result obtained above encouraged using ACD half section as feed for 200 Ω IRA design and ACD full section as feed for 100 Ω IRA. Two ACD plates of length 184 mm and 2 mm thickness were connected in parallel at the feed point to get an input impedance of nearly half the value of the individual dipoles. The combined arms were rotated around the feed point towards the reflector and four terminating resistors each of 200 Ω is placed between dipole end and reflector as shown in Fig. 10. The ACD plate is aligned $\pm 30^\circ$ from the vertical axis for the new designs. The new IRA using feed as half ACD section and the conventional IRA of 200 Ω input impedance is analyzed using the same gaussian excitation signal of source impedance of 200 Ω and the other simulation conditions remain same. The calculated return loss plot of the new and conventional IRA as shown in Fig. 12. shows that new half ACD feed IRA provide good impedance matching up to 15GHz. Time domain far-zone electric field calculated at bore sight of the new and conventional IRA is shown in Fig. 14. XFDTD (v7.1) solver calculates the far-zone electric field at infinity and normalizes it to $|r| = 1$ m. The temporal characteristics of new IRA are comparable to the conventional IRA but peak electric field of new IRA is larger than conventional IRA at the bore sight.

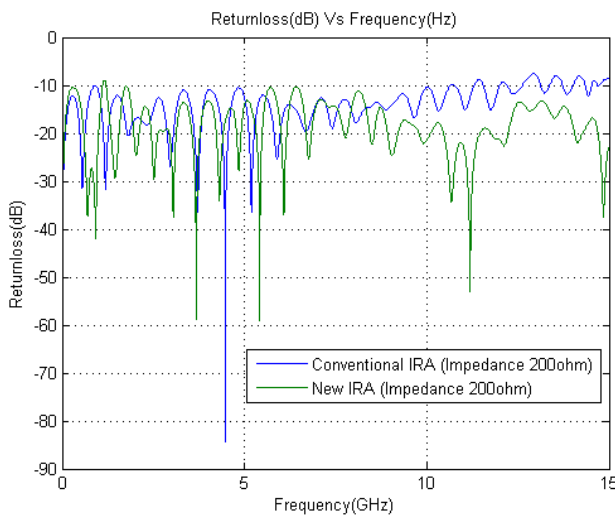


Fig. 12 Return loss (dB) Vs Frequency (GHz)

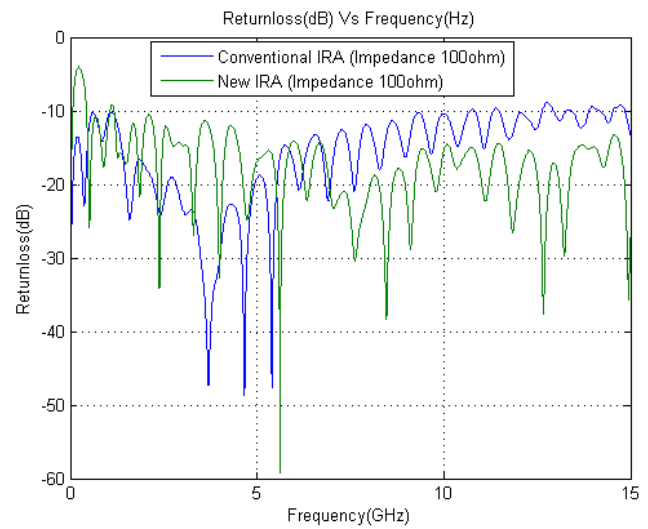


Fig. 13 Return loss (dB) Vs Frequency (GHz)

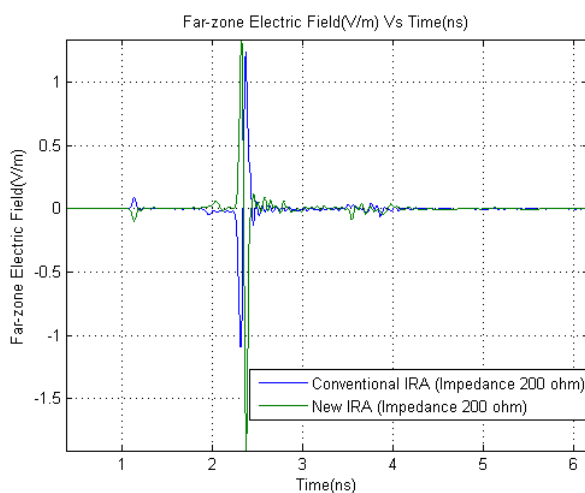


Fig. 14 Far-zone Electric field of Conventional & New IRAs

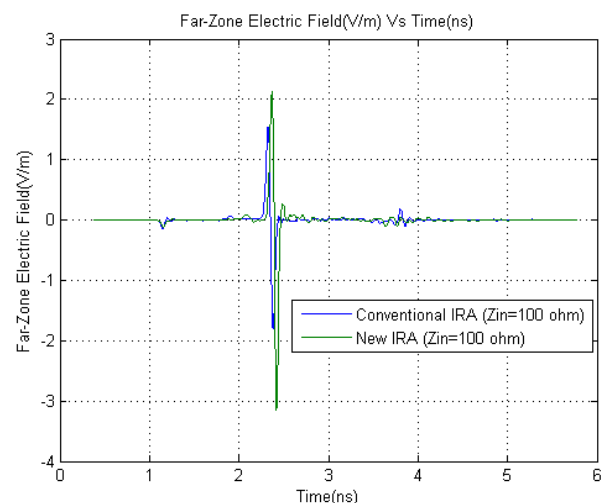


Fig. 15 Far-zone field of Conventional & New IRAs

The gain at bore sight of the new IRA is more than 4 dB higher compared to conventional IRA in higher frequencies as shown in Fig. 16. New IRA of reduced input impedance of 100Ω is designed with full ACD plate of length 184 mm and 2 mm thickness and a 46 cm diameter parabolic reflector with focal length 18.4 cm as shown in Fig. 11. Feed arms are placed at $\pm 30^\circ$ from the vertical axis and the terminating resistors of 100Ω are placed between each arm ends and the reflector. New reduced impedance IRA (Fig. 11) and conventional IRA (Fig. 4) of input impedance 100Ω is analyzed in time domain using XFDTD (v7.1) using the same gaussian excitation pulse of source impedance 100Ω with other simulation condition remains same.

The calculated return loss plot for new and convention IRA is shown in Fig. 13. This plot shows that new IRA offers good impedance matching from 500 MHz to 15 GHz. The time domain far-zone electric field at bore sight for new and conventional IRA is shown in Fig. 15. The peak electric field observed for new IRA is larger than convention IRA. The gain in bore sight direction for new IRA is more than 3 dB higher compared to convention IRA in most of the high frequency range as shown in Fig. 17. The FDTD analysis of conventional and new IRAs of both impedance categories shows the edge of new IRA over conventional IRA. The new feed becomes very useful particularly for reduced impedance IRA design because of its slimmer profile compared to conventional conical taper line.

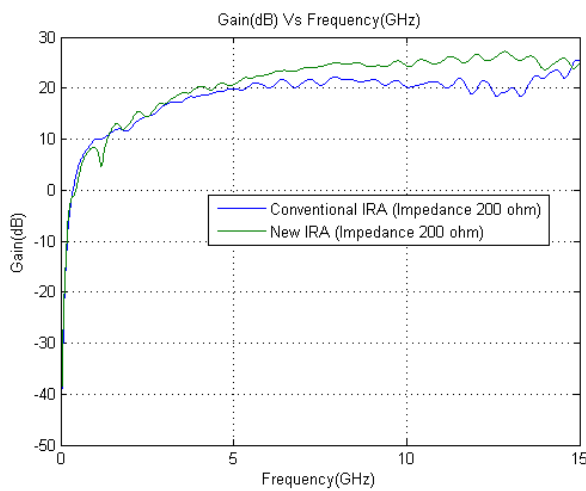


Fig. 16 Gain of Conventional & New IRAs at bore sight

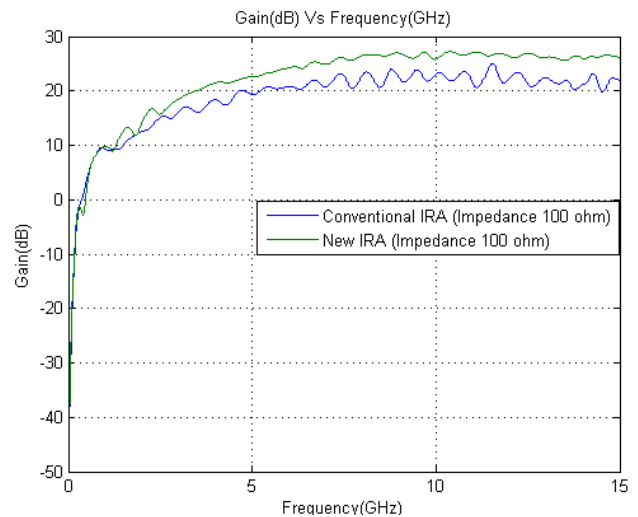


Fig. 17 Gain of Conventional & New IRAs at bore sight

The normalized impulse response of the antenna is calculated using transmission relation A.1 discussed in [13].

$$\frac{E_{rad}(t)}{\sqrt{377\Omega}} = \frac{1}{2\pi cr} h_N(t) \circ \frac{dV_{ex}(t)/dt}{\sqrt{Z_{in}}} \quad (3)$$

Where, $E_{rad}(t)$ is radiated electric field at distance r from the antenna and $V_{ex}(t)$ is excitation signal used for time domain simulation, Z_{in} is the input impedance of the concerned IRA and $h_N(t)$ is the normalized impulse response of the IRA.

The excitation voltage source $V_{ex}(t)$ used for FDTD simulation for different antennas remains same as shown in Fig.8. and the $E_{rad}(t)$ data in bore sight direction is obtained from FDTD simulation for different antennas used to calculate $h_N(t)$ for different IRAs. The normalized impulse response $h_N(t)$ of the antenna is calculated using Fourier transforms and simplified Butterworth filter as suggested in [13]. The normalized impulse response for conventional and new IRA of 200Ω and 100Ω input impedance categories are shown in Fig.18 and Fig.19 respectively. The pulse width of the impulse response of both new and conventional IRA is comparable for both input impedance categories. The peak amplitude of new IRA is larger than conventional IRA for both input impedance categories. The late time ringing observed in the normalized impulse response in both cases is may be due to implementation issues of the filter.

The time domain reflectometry (TDR) of all the four designs is calculated from their reflection coefficient data obtained from the simulation. The TDR of conventional and new IRA for 200Ω and 100Ω input impedance is shown in Fig.20 and Fig.21 respectively. The excitation source is directly connected at the apex of the TEM line with necessary source impedance without any cable or balun in the case FDTD analysis. The TDR plot in both the figures starts from the apex of the TEM feed line.

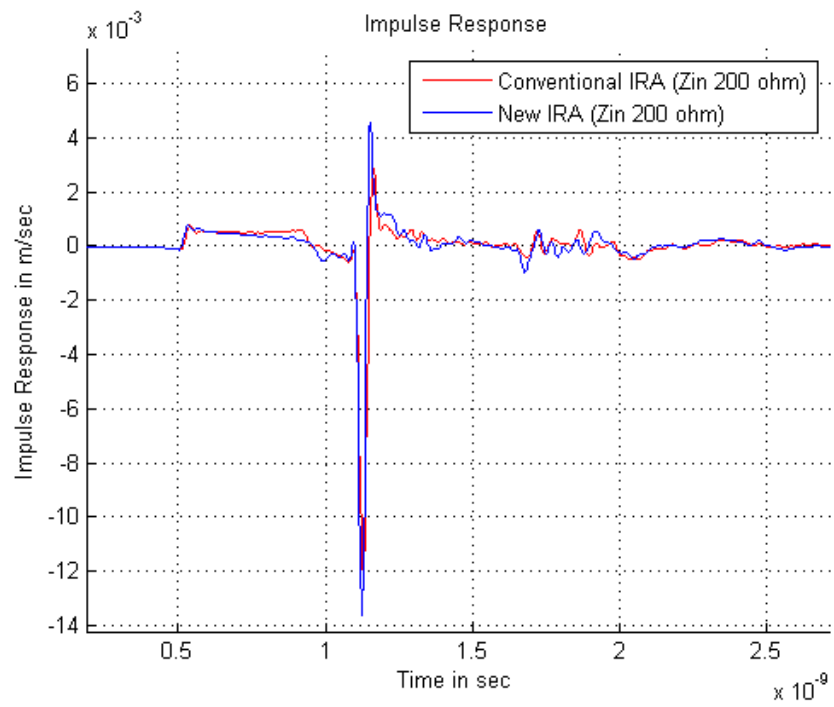


Fig. 18 Normalized impulse response of Conventional and New IRA at Bore sight

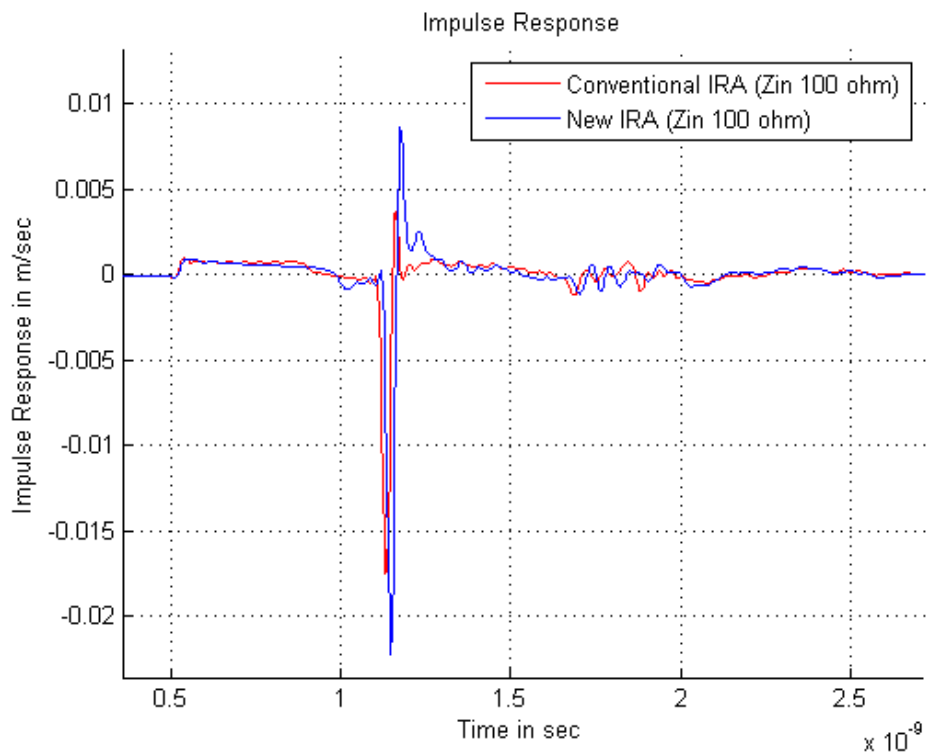


Fig. 19 Normalized impulse response of Conventional and New IRA at Bore sight

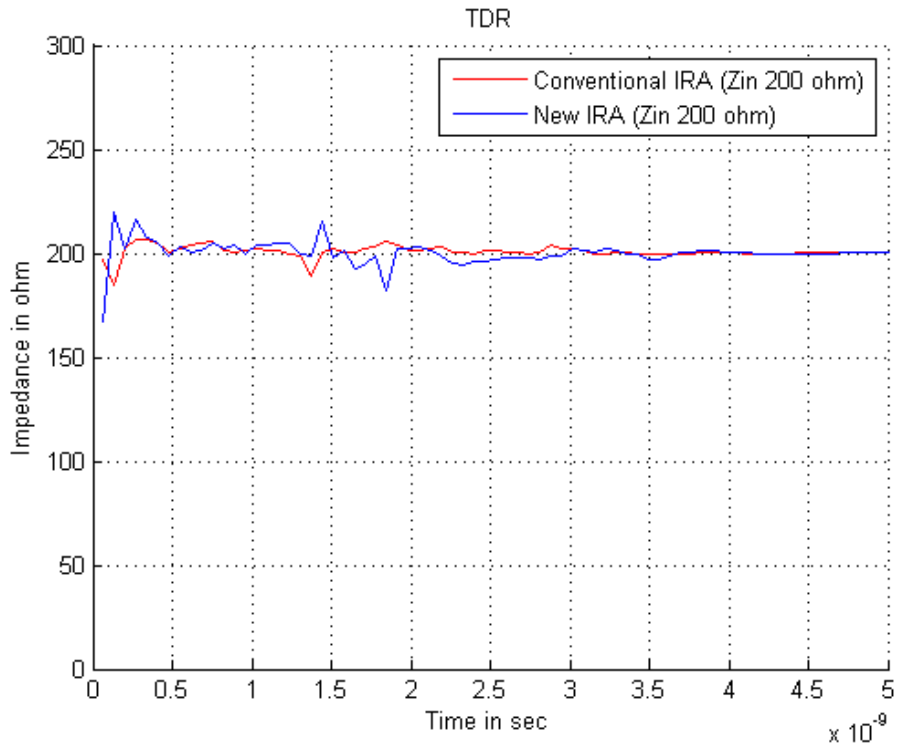


Fig. 20 TDR of Conventional and New IRA (Zin 200Ω)

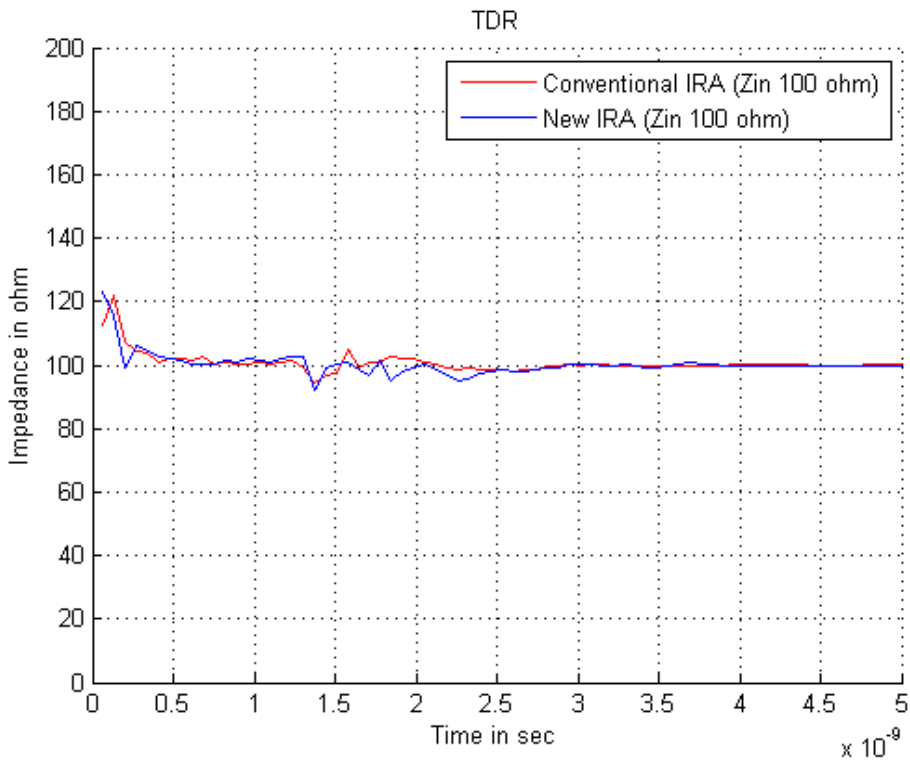


Fig. 21 TDR of Conventional and New IRA (Zin 100Ω)

The new IRA of 100 Ω input impedance is further reduced to half reflector with two arms and ground

plane making it a half IRA (HIRA) with input impedance 50Ω to connect to standard instrumentations for measurement. The realized new HIRA is shown in Fig. 22. The 100Ω terminating resistor is realized using 20 mils thick RT/Duroid 5870 with Nickel-Phosphorous resistive material instead of discrete resistors as shown in Fig. 22. Embedded resistors along with the Teflon support is used at each arm end to reduce lead inductance of discrete resistors.

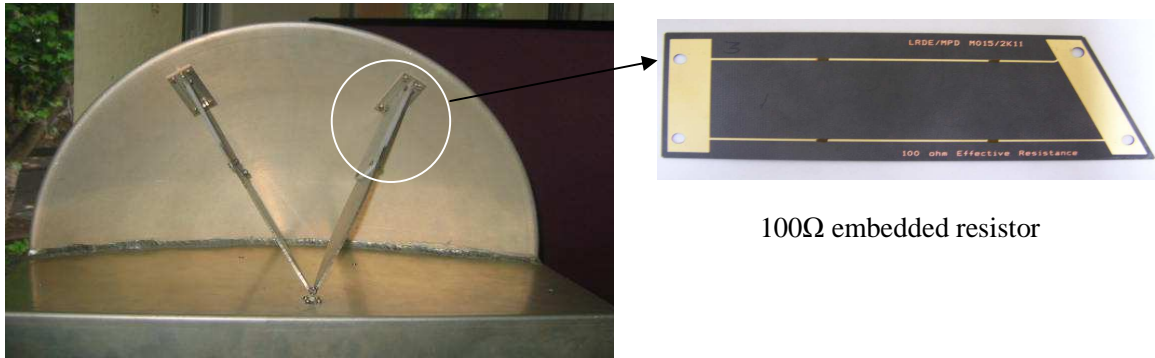


Fig. 22 Realized New HIRA

The gain of the new HIRA was measured in near field antenna test facility on some of the spot frequencies from 500 MHz to 15 GHz is shown in Fig. 23. The measured input impedance of the new HIRA is shown in Fig. 24. The measured result shows that the antenna has good impedance matching in the frequency range 500 MHz to 15 GHz. The time domain response of new HIRA is measured using measurement setup [15] consists of an UWB arbitrary wave generator (AWG) (Tektronix AWG 7122C), an Oscilloscope (Tektronix TDS71604 DPO 16 GHz), ACD sensor (prodyn AD-70D) and balun (prodyn BIB-100F). The input excitation pulse used for antenna evaluation is a gaussian derivative pulse as shown in Fig. 25. The measured time domain response of the new HIRA is first time derivative of the input excitation pulse as shown in Fig. 26. The different antenna parameters, which defines figure of merit of this class of antennas [10] is discussed in [15] for the new IRA design. The TDR response of the new HIRA as shown in Fig. 27 is calculated from measured return loss data.

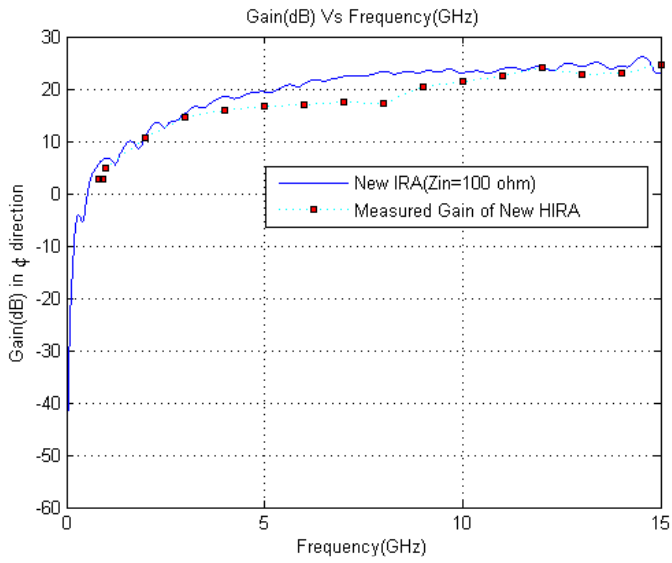


Fig. 23 Measured gain of New HIRA

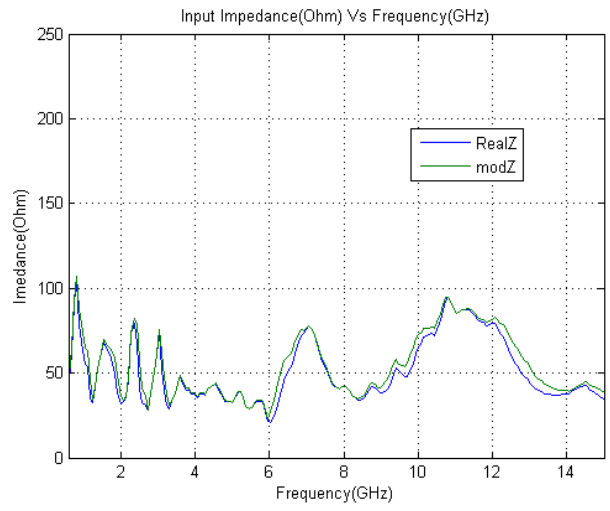


Fig. 24 Measured input impedance of New HIRA

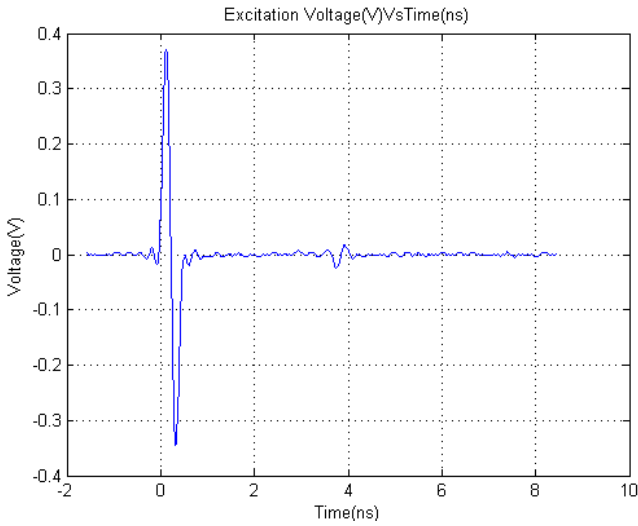


Fig. 25 Excitation signal used for time domain measurement

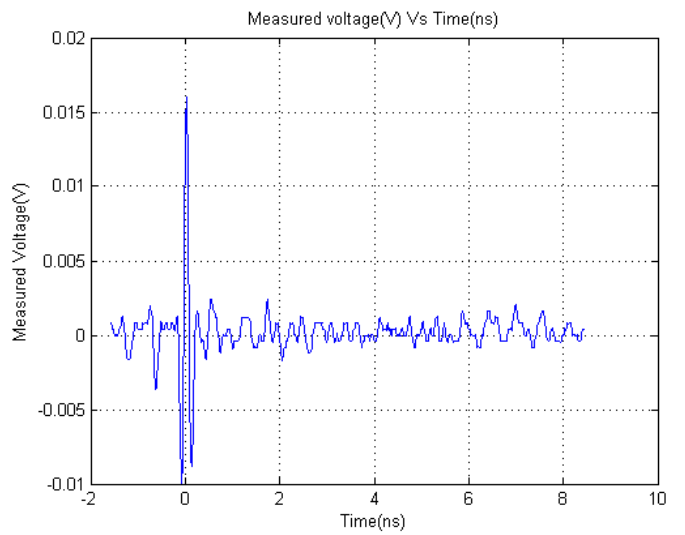


Fig. 26 Measured time domain response of new HIRA

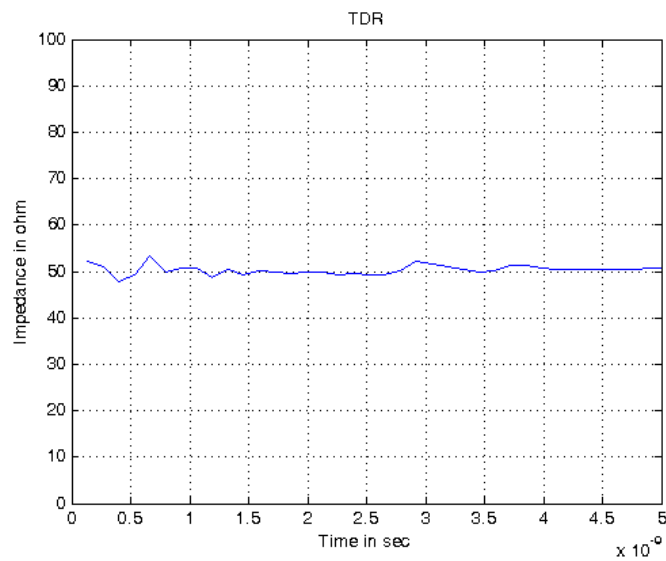


Fig. 27 TDR response of new HIRA

5. DISCUSSION

Asymptotic conical profiles obtained using different charge distributions discussed in [15] shows its application as an UWB dipole antenna as well as feed for reflector IRA. Four different designs of reflector IRAs with conventional feed as well as ACD feed for both $200\ \Omega$ and $100\ \Omega$ categories is presented here. The FDTD analysis results shows that New IRAs offers more than 4 dB gain in higher frequencies compared to Conventional IRAs for both $200\ \Omega$ and $100\ \Omega$ category. New IRAs offers a slimmer profile hence reduced weight specially for $100\ \Omega$ category. The $100\ \Omega$ new IRA was reduced to HIRA to get $50\ \Omega$ input impedance of the antenna for measurement with standard instrumentations without any adaptor. The analysis and measurement results show that new IRAs can be a better choice for both time domain as well as frequency domain applications.

6. CONCLUSION

The New IRAs shows good time domain as well as frequency domain response compared to conventional IRAs for both $200\ \Omega$ and $100\ \Omega$ category. The input impedance of the antenna is brought down to nearly half across the frequency band by using full section of ACD and further antenna was reduced to HIRA to get nearly $50\ \Omega$ for connecting to the standard measurement instrumentations. These ACD feed arms offers ultra wideband characteristics and have slimmer profile than conventional conical line for respective characteristic impedance. The new IRA offers a good solution for reduced input impedance requirements

and new HIRA can be widely used for many UWB applications, as it does not need any impedance adaptor for connecting with standard measurement instrumentations.

REFERENCES

1. DuHamel R.H et al., "Frequency independent conical feeds for lens and reflectors", in *proc. IEEE Int. Antennas Propagation Symp.* Dig.Vol.6, Sep.1968, pp. 414-418.
2. Baum,C.E., "Radiation of Impulse-like Transient Fields", *Sensor and Simulation Notes* 321, 25 November 1989.
3. Baum,C.E., and E.G. Farr, "Impulse Radiating Antennas", in *Ultra-wideband Short Pulse Electromagnetics*, edited by H.L Bertoni et. al., pp. 139-147, Plenum Press, NY 1993.
4. Baum,C E., "Configuration of TEM Feed for IRA", *Sensor and Simulation Notes* 327, 27 April 1991.
5. Farr,E., "Optimizing the feed Impedance of Impulse Radiating Antenna,PartI: Reflector IRA", *Sensor and Simulation Notes* 354, January 1993.
6. Farr.E et al., "Prepulse associated with the TEM feed of an Impulse Radiating Antenna", *Sensor and Simulation Notes* 337, March 1992.
7. M.Manteghi and Y.Rahmat-Samii, "A novel Vivaldi fed reflector impulse radiating antenna (IRA)," in *Proc. IEEE Int. Symp. Antennas and Propagation*, Washington,DC, Jul.3-8,2005, pp. 549-552.
8. M.Manteghi and Y.Rahmat-Samii, "On the characterization of a reflector impulse radiating antenna (IRA): Full-wave analysis and measurement results", *IEEE Trans. Antennas and Propagation*, Vol.54, no.3, pp. 812-822, Mar 2006.
9. L. H Bowen et al., "A high voltage Cable feed impulse radiating antenna", in *Ultrawideband short pulse electromagnetics8*, edited by Baum et al., pp. 9-16, Springer, 2007.
10. D.V.Giri, "Peak Power Gain in time domain of Impulse Radiating Antenna (IRAs)", *Sensor and Simulation Notes* 546, October 2009.
11. Sower G.D., "Optimization of the asymptotic conical EMP sensors", *Sensor and Simulation Notes* 295, Oct 1986.
12. C.E.Baum, "An equivalent charge method for defining geometries of dipole antennas", *Sensor and Simulation Notes* 72, Jan 1969.
13. Lanney M Atchley et al., " Characterization of Time Domain Antenna Range", *Sensor and Simulation Notes* 475,June 2003.
14. Dhiraj Kumar Singh, D C Pande, and A. Bhattacharya, "A new feed for Reflector based 100 Ω Impulse Radiating Antenna", *PIERS 2012*, Malaysia, Mar 2012.
15. Dhiraj Kumar Singh, D C Pande, and A. Bhattacharya, "Selection of ideal feed profile for Asymptotic conical dipole fed impulse radiating Antenna", *Sensor and Simulation Notes* 563, June 2013.